19th Brazilian Congress of Thermal Sciences and Engineering
November 06th-10th, 2022, Bento Gonçalves - RS - Brazil

ENC-2022-0142
THERMOHYDRAULIC PERFORMANCE OF NANOFLUID FLOW WITH SUDDEN GEOMETRY CHANGE

Felipe Silva dos Santos[1]
Enio Pedone Bandarra Filho[2]
Mohammad Reza Safaei[3]
Federal University of Uberlandia (UFU), School of Mechanical Engineering, Av. Joao Naves de Ávila, 2121 – Santa Monica, Uberlandia, MG 38400-902, Brazil[1,2]
Florida International University, Department of Civil and Environmental Engineering, Miami, Florida, U.S.A[3]
phelipe.moutinho@gmail.com[1]
bandarra@ufu.br[2]
cfd_safaei@yahoo.com[3]

Abstract. *Application of nanofluids in heat transfer enhancement is growing significantly since this new technology is well-suited to heat transfer processes. Several studies on the effect of nanofluids in heat transfer have been conducted to determine the enhancement of properties in addition to rearrangement of flow passage configurations. The main objective of this research is evaluating the performance of nanofluid in single-phase flow with geometry change in heat transfer systems for engineering applications. A test rig was developed to evaluate nanofluids flowing inside tubes focusing on heat transfer and pressure drop. The nanofluids used in the current study, multi-walled carbon nanotube (MWCNT) was produced using the ultrasound as the dispersal mechanism by the two-step method and the measurement of the thermophysical properties (specific mass, viscosity, and thermal conductivity) of the produced nanofluids was also performed. The tests were performed at steady-state condition, and all the inlet parameters were varied: geometry of the test section, inlet temperature in the test section, the flow of the working fluid, supplied heat flux, types of nanofluids, and mass fraction of nanoparticles, etc. At this stage, the experimental data were compared with mathematical models and correlations proposed in the literature to predict thermophysical properties of nanofluids and parameters related to the process of heat transfer by convection. The results indicated that the Reynolds number and the volumetric fraction of nanoparticles affect the heat transfer coefficient considerably; an increase in the local heat transfer coefficient was observed when both the Reynolds number and the volume fractions of nanoparticles are increased for all cases. Therefore, at a constant Reynolds number, the increase in heat flux had no significant influence on the heat transfer and fluid flow parameters.*

Keywords: *Nanofluid, heat transfer, sudden geometry change.*

1. INTRODUCTION

The study of heat transfer and nanofluid flow in circular tubes using numerical and experimental approach are primarily investigated by many authors such as (Salman et al., 2013), (Hoffmann, 2014), (Hosseinian et al., 2018), (Cárdenas Gómez, 2019) and (Dadhich et al., 2020). However fewer researchers have considered the effects of sudden contraction /expansion in heat transfer and pressure drop of nanofluid flow.

Flows through a sudden axisymmetric contraction or expansion, in forward facing step (FFS) or backward facing step (BFS) channels and through channels with obstacles, create separation and subsequent reattachment zones (Kazi and Togun, 2015). Separation and recirculation zones have a significant impact on the performance of heat exchangers, electronic cooling systems, automotive radiators, microchannels, circular ducts, and other heat transfer equipment, which is considered in engineering projects. As a result, the reattachment zone mixes a considerable amount of low and high energy (Salman et al., 2020).

The separation region is followed by turbulent structures that affect the heat transfer performance of the nanofluid, as observed by several researchers in numerical and experimental works (Abdulrazzaq et al., 2020; Amiri et al., 2016; Kimouche et al., 2017; Qi et al., 2020). Hilo et al. (2020) experimentally investigated the forced convection heat transfer and friction factor in nanofluid flow in BFS channels with ER equal to 2, the authors reported that the heat

transfer increases with increasing nanoparticle volume concentration, where the Nusselt number increased by 11 % at a volume concentration of 0.05 of CuO and MgO compared to pure ethylene glycol (EG), and the friction factor increased by approximately 15 % with a Reynolds equal to 5000 and volume concentrations of 0.01 and 0.03.

Togun et al. (2017) investigated numerically and experimentally the heat transfer in nanofluid flow on turbulent regime in a concentric annular pipe with different sudden expansion ratios. The authors used the Al2O3/Water nanofluid in the material experiment to validate the results of the computational model. For an expansion ratio of 2, volume concentration of 2%, and Reynolds number of 50000 the average increase in the heat transfer coefficient for the Al2O3/Water nanofluid was approximately 6.59 % for the material experiment and approximately 6.48 % for the computational experiment, indicating good agreement between the numerical and experimental results. Hilo et al. (2020) experimentally investigated the convective heat transfer in a BFS channel of nanofluid flow under uniform heat flux. The authors reported an 11 % increase in the Nusselt number for the CuO/Ethylene glycol (EG) nanofluid with a volumetric nanoparticle concentration of 5 % relative to the base fluid. EG. Montazer et al. (2020) experimentally investigated heat transfer with forced convection in the turbulent regime for nanofluid flow in a heat exchanger with axisymmetric sudden expansion. The authors presented two correlations for the local Nusselt number, which increased with increasing axial radii in all investigated cases. The authors reported that among all investigated nanofluids, those with carbon-based nanoparticles had a greater effect on increasing the heat transfer (33.7 % and 16.7 % for F-GNP functionalized graphene nanoplatelets and MWCNT multi-walled carbon nanotubes respectively at a mass concentration of 0.1 %) downstream of the sudden expansion in the pipe.

Kherbeet et al. (2015) numerically and experimentally investigated the heat energy transfer characteristics in horizontal flow of nanofluids in microchannels with forward facing step (MFFS). The authors considered two types of nanofluids were considered, SiO_2/Water and Al_2O_3/Water as well as pure water. They reported with the experimental results that compared to pure water, the largest increment in Nusselt number was 30.6 % for the SiO_2/Water nanofluid with a volume concentration of 1 %.

Abdulrazzaq et al. (2020) numerically and experimentally investigated the turbulent flow of Al_2O_3/Water and TiO_2/Water nanofluids in an annular pipe with sudden contraction and in another one without geometry change. The authors reported that the maximum increase in thermal performance was 194.6 % in the annular channel with contraction ratio equal to two compared to the straight pipe. The authors attributed the increase in heat transfer to the recirculation zone and the downstream flow separation region. It was also reported that among the investigated nanofluids Al_2O_3/Water with a volume concentration of 2 % showed the best thermal performance.

Works involving expanding/contracting nanofluid flow on heat energy transfer in nanofluids considering geometry change effects are quite limited, with the vast majority of works on this topic performed numerically. The key results of the main experimental studies are presented in Table 1, where the researchers mainly focused on the analysis of Nusselt number and heat transfer coefficient for different nanofluids.

Table 1. Summary of the state-of-the-art involving heat transfer contraction/expansion nanofluid flow.

Author	**Nanofluid**	**Contraction/expansion ratio**	**Findings**
Kherbeet et al. (2014)*****	Al_2O_3/Water SiO_2 / Water	2	For Al_2O_3 and φ = 1 % h ↑ 22.1 % For SiO_2 and φ = 1 % h ↑ 30.6 %
Amiri et al. (2016)******	EGGNP/Water:Ethylene glycol (40:60)	2	h ↑ 25.88 % Nu ↑ 26.05 %
H. Togun et al. (2017)**	Al2O3/Water	1.25; 1.67; 2	For Al2O3 and CR = 2 h ↑ 6.59 %
A.K. Hilo et al. (2020)**	CuO/EG MgO/EG	2	For CuO Nu ↑ 11 % For MgO Nu ↑ 5.4 %
E. Montazer et al. (2020)**	GNP /DW MWCNT/DW SiO_2/DW ZnO/DW	2	For GNP h ↑ 33.7 % For MWCNT h ↑ 16.7 % For ZnO h ↑ 14.35 % For SiO2 h ↑ 10.1 %
T. Abdulrazzaq et al. (2020)*	Al_2O_3/DW	2	For Al_2O_3 and CR = 2 he ↑ 20.62
D. Yang et al. (2021)**	TiO_2/DW SiO_2/DW Al_2O_3/DW	2 (microchannels)	For TiO2 Nu ↑ 28 % For SiO2 Nu ↑ 25 % For Al2O3 Nu ↑ 48 %
Talib and Salman (2022)**	βGa_2O_3 / Water	2 (MBFS)	βGa2O3 and φ = 4 vol. % Nu ↑ 19.2 %

*Contraction ratio; **Expansion ratio

2. EXPERIMENTAL PROCEDURE

The samples of nanofluids were realized using two-step method. The nanoparticles were acquired in powder of a functionalized solution in high weight concentration and scattered in two types of base fluids. The first is a mixture of water and ethylene glycol with 50% of mass concentration of each substance (H_2O:EG 50:50% wt.).

2.1 Nanofluids based on water and ethylene glycol (H_2O:EG 50:50% wt.)

To produce the nanofluids based on water and ethylene glycol (H_2O:EG 50:50% wt.), a routine described in Fig. 1 was established. Were used nanoparticles of two different categories of base materials; nanoparticles based on carbon (carbon nanotubes) and nanoparticles based on inorganic materials (metal), with multi-walled carbon nanotube (MWCNT).

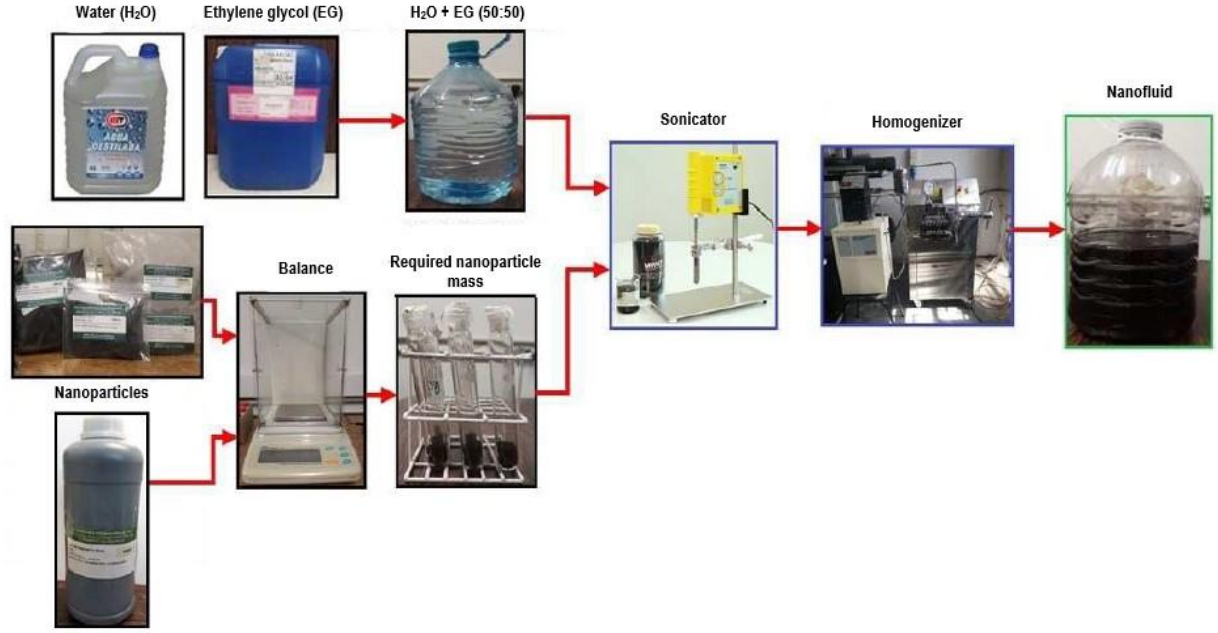

Figure 1. Nanofluid production process.

Therefore the samples of nanofluids produced were the result of a process of dispersion, sonication and homogenization of nanoparticles in powder form or a functionalized solution of high concentration in mass of nanoparticle. Both powdered nanoparticles and functionalized solution of high concentration based on water supplied by Nanostructures & Amorphous Material, where the physical properties (specific mass and specific heat) and the geometric and morphological characteristics were provided by the manufacturer.

Table 2 shows the main properties of the samples produced as base fluid and mass concentration. To determine the amount of mass of nanoparticles a routine was developed in the EES software. In this sense, the desired volumetric concentration for each nanofluid and the final volume (V_f = 3500 ml) were previously defined.

Table 2. Description of nanofluid samples produced.

Sample	Base fluid	[% mass] wt.
MWCNT	H_2O:EG 50:50% wt.	0.005 0.01 0.05

2.2 Stability analysis

The stability of MWCNT/H2O-EG nanofluid was studied by obtaining the optical absorption spectra using the UV-Vis spectroscopy. The peaks of wavelength ranging from 400-1100 nm were used to obtain the relationship of absorbance and mass concentration. A wavelength of 400 nm was used of reference value to show the relation between

mass concentration and absorbance of samples, as can be seen how much higher the mass concentration, grater its absorbance. Fig. 2 shows the obtained values after preparation of samples. It was noted a linear relation between absorbance and mass concentration as reported by Swinehart (1962).

Fig. 3 shows the results of UV-Vis spectroscopy in a reference wavelength value of 400 nm for relative mass concentration obtained of a regression by figure 2 in relation to different times of measurement. As can be observed the mass concentration decrease as time goes on, it happens probably due the decanting of samples, which leads to a decrease in absorbance over time.

UV–vis spectroscopy is used to quantitatively characterize the stability of the dispersion of nanofluids samples due the easy visualization of wavelength decrement during the time. How much lower the wavelength decrease more stable is the nanofluid samples.

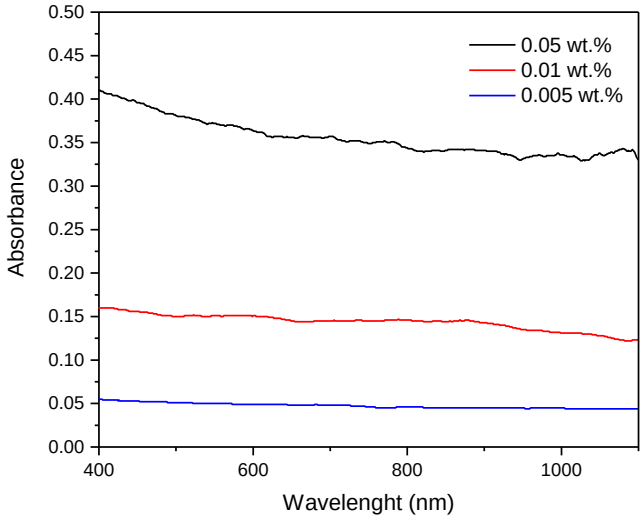

Figure 2. Relationship between absorbance and wavelength for nanofluid samples.

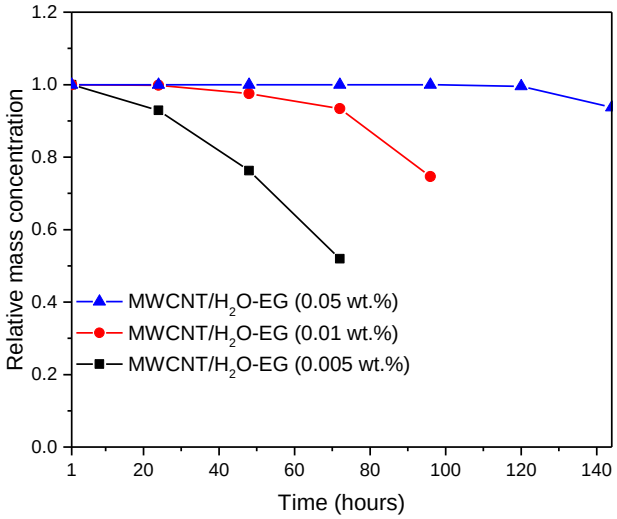

Figure 3. Relative wavelength of MWCNT/H2O-EG nanofluid in relation to different times of measurements.

2.3 Morphological characterization

The morphology of the nanoparticles was obtained by SEM and MET images. SEM images are not able to show in detail the surface of the nanoparticles due to the lack of sharpness with the large application, so they were made aiming to show the characteristic shape of shape of each nanoparticle. On the other hand, MET images are more accurate and able to show the multiple walls of carbon nanotubes, depending on the equipment used. Fig. 4 (a-b) show the SEM and TEM images of MWCNT nanoparticles investigated.

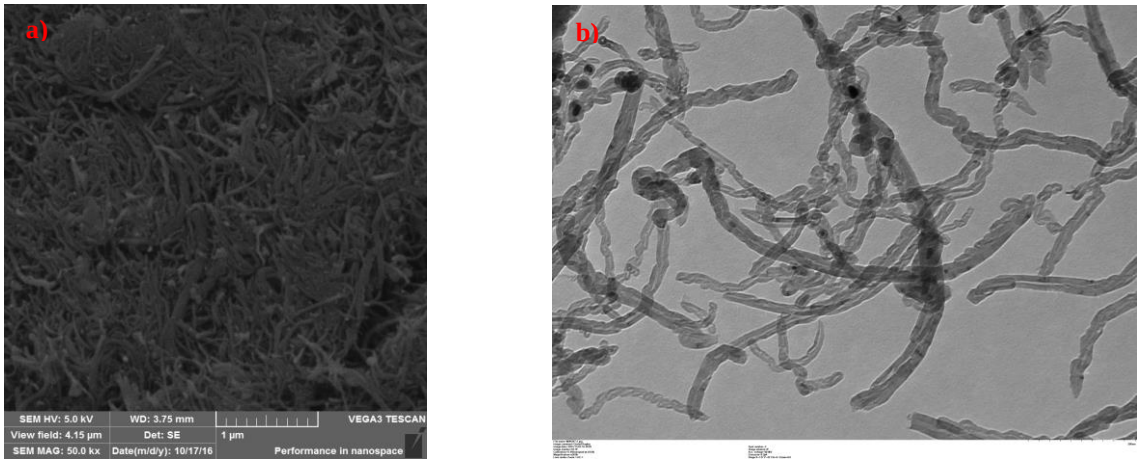

Figure 4. a) SEM image of MWCNT nanoparticles; b) TEM image of MWCNT nanoparticles

The effects of the number of walls, inner and outer diameters, and the presence of a defect on the structure of CNTs regarding their mechanical properties or even on the improvement in the mechanical properties of the metal matrices are not entirely understood. Although the morphology and structure affect the mechanical properties of CNTs, the success of reinforcement of metallic matrices also depends on other factors, such as a good dispersion of CNTs, a strong interface bonding between the reinforcement and the matrix, and even the possibility of reaction between the matrix and reinforcement. In this sense, it is important to identify and understand how the morphology and structure of CNTs can affect the mechanical properties of nanocomposites, but also to determine whether these characteristics can affect other key factors in the production of these nanocomposites. To evaluate and validate the effect of the morphology and structure of CNTs on the production of nanocomposites, different MWCNTs were used as reinforcement materials (Carneiro and Simões, 2020).

2.4 Thermophysical properties

In this work, the thermal conductivity was measured by the conductivimeter LINSEIS, model THB-1, it is based in the hot transient bridge technique, which allows the measurement of thermal conductivity, thermal diffusivity, and specific heat of various materials as solids, liquids, powders, and pastes. The measurement is automatic and did by the software provide by the manufacturer with 10 measurements per cycle and 2 to 3 cycles per sample. The range of temperatures used was 20 °C to 50 °C. Table 3 show the Measuring ranges in detail.

Table 3. Specifications of THB-1 LINSEIS provided by manufacturer.

Parameter	Temperature range	Measurement range	Measurement uncertainty
Thermal conductivity	20 °C to 50 °C	0.01 to 1 W/(mK)	Better than 2 %
Thermal diffusivity		0.05 to 10 mm^2/s	Better than 5 %
Specific heat		100 to 5000 $kJ/(m^3K)$	Better than 5 %

The temperature range used was 20 °C to 50 °C. The final value of conductivity was the arithmetic mean of results obtained, eliminating discrepant results.

The dynamic viscosity as well as the density of the nanofluids were measured on a rotational viscometer, model Stabinger™ SVM™ 3000, from Anton Paar, which has a cylindrical geometry with concentric tubes. The temperature was controlled by the equipment using a range 20 °C to 80 °C. The samples were injected in the equipment, and the calculation of the dynamic viscosity did from the rotor speed. Simultaneously the equipment obtained values of dynamic viscosity, viscosity kinematics and specific mass. Table 4 presented the uncertainty measurements of viscosity, specific mass and temperature and its repeatability.

Table 4. Uncertainty data of Anton Paar viscometer measurement.

Parameter	Temperature range	Measurement range	Measurement uncertainty
Dynamic viscosity	20 °C to 80 °C	± 0.35 %	± 0.1 % of measured value
Density		± 0.0005 %	± 0.0002 g/cm^3
Temperature		± 0.02 %	± 0.0005 °C

2.5 Experimental rig

The test rig was modified to ensure specific requirements for the proposed research, improving the control and monitoring system of the variables of interest and shifting the test section's geometry. Also, periodic calibration of the instruments was necessary to ensure greater reliability of the results obtained through these instruments. The current model of the test rig available is shown in Fig. 5a and 5b where the test section is a straight pipe through which nanofluid flow with heat transfer occurs, Fig. 6 shows the proposed modifications for the test section with contraction.

During this stage, the test rig's validation was addressed, which was performed using the chosen nanofluid, thermal oil, distilled water, or other reference fluid in the test section. This stage aims at knowing the experimental limits of the system operation, the closing of the energy balance, the analysis of experimental uncertainties and the selection of test conditions.

With the test rig instrumented and available for testing, the next step was to implement the methodology for determining the convective heat transfer coefficient and the friction factor. However, the experimental procedure and the analysis of the data obtained from the test rig, were initially validated using distilled water-ethylene glycol mixture (H2O:EG 50:50 wt.%) as test fluid, since there is consolidated information in the literature describing their thermohydraulic behavior. The purpose of the validation is to ensure that the experimental equipment can perform, consistently and correctly, all measurements initially for the base fluid and later for the nanofluid.

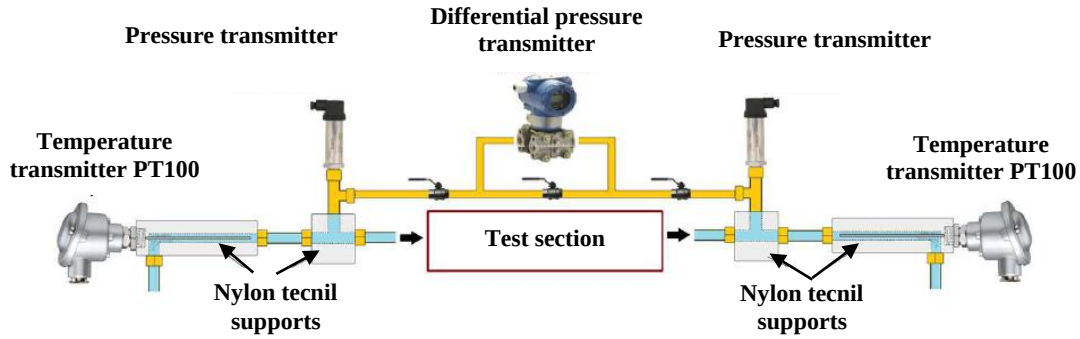

(a)

(b)

Figure 5. (a) Structural layout of installing the measuring instruments in the test section. (b) Physical model of current test section. Source: (Author's own).

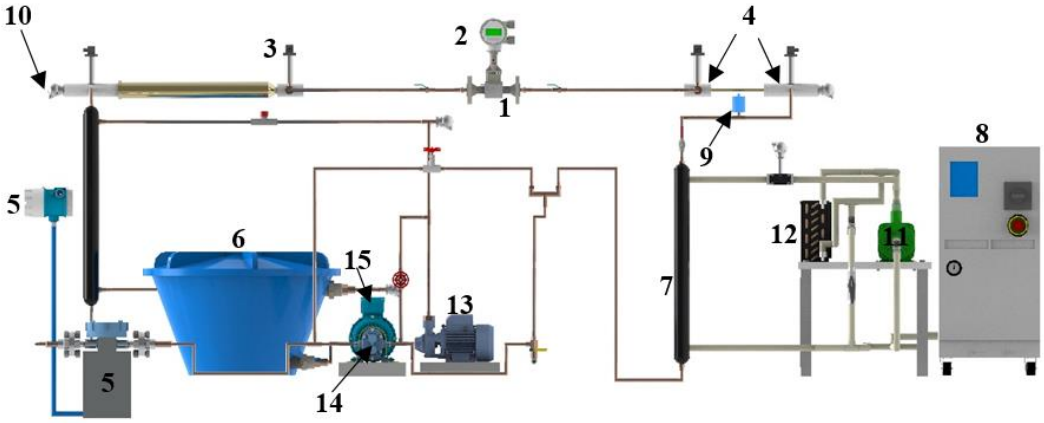

Figure 6. Modified test section on the test rig for expansion flow. 1: Test section; 2: Differential pressure transmitter; 3: Pressure transmitter; 4: Nylon tecnil supports; 5: Coriolis; 6: Preheating system; 7: Heat exchanger; 8: Water chiller; 9: Nanofluid reservoir; 10: Temperature transmitter; 11: Water pump; 12: Condensing unit; 13: Water pump; 14: Gear pump; 15: Electric motor. Source: (Author's own).

3. EXPERIMENTAL RESULTS

This section presents the experimental results of thermal conductivity, density, and dynamic viscosity measurements for MWCNT/H2O-EG nanofluid. A comparison with the physical properties of the theoretical base fluid was made for different temperature ranges in all analyzed cases. Fig. 7 and Fig 8 shown the results of dynamic viscosity and density for nanofluid using a temperature range of 20 °C-80 °C.

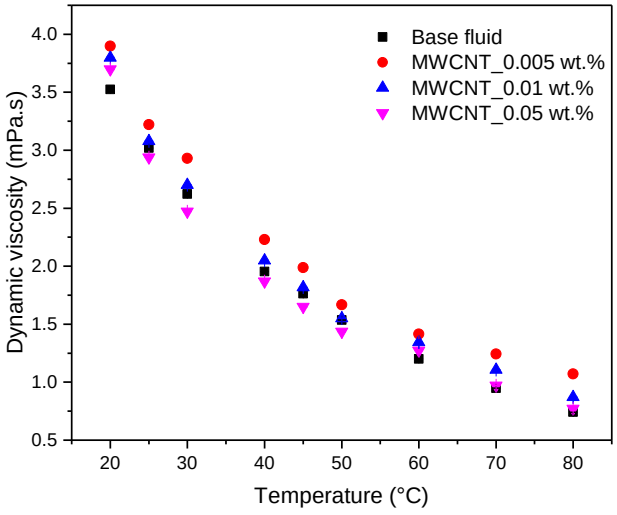

Figure 7. Comparison between experimental results for dynamic viscosity of nanofluid samples and base fluid.

In Fig. 7 we can see that the nanofluids samples present dynamic viscosity values higher than base fluid, where viscosity increments obtained for nanofluids samples of carbon nanotubes with aspect ratio (r=l/d=800) were on average 4.68 %, 7.19 % and 9.58 % for samples of MWCNT/H2O-EG with nanoparticle mass concentration of 0.005 %, 0.01 % and 0.05 % respectively. The absorbed water layer can be formed around the nanoparticles in nanofluids, which increases the equivalent radius of nanoparticles. Higher interfacial resistance will form for higher surface area, which will hinder the mobility of the nanoparticles in base fluid, causing the increase in the viscosity (Zhang and Han (2018)).

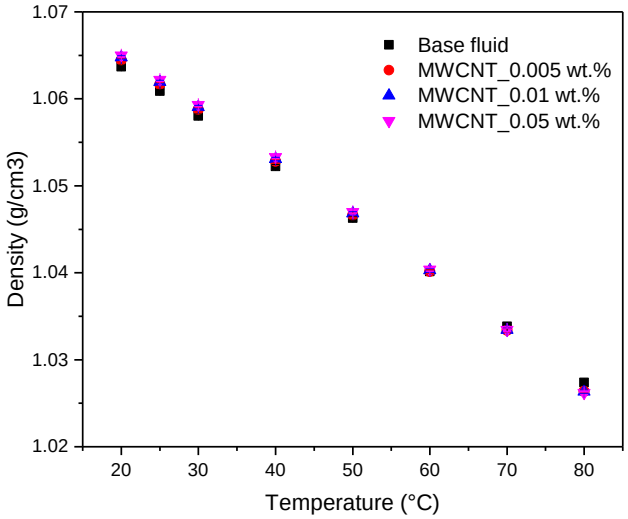

Figure 8. Comparison between experimental results for density of nanofluid samples and base fluid.

In Fig. 8 we can be see a slight increment of the density of nanofluid samples in relation to base fluid. The maximum increments obtained for nanofluid samples of MWCNT/H2O-EG in relation to base fluid were on average 0.07 %, 0.1 % and 0.12 % for nanofluid samples with mass concentration of 0.005 wt.%, 0.01 wt.% and 0.05 wt.% respectively. Due the attraction of van de Waals force existed among the particles of nanofluids, the nanoparticles are inclined to gather to form aggregate in nanofluids, and when the mass fraction of the nanoparticles in the nanofluids increase, the quantity of the nanoparticles will increase too, thus the nanoparticle tend to form bigger aggregate in the nanofluids.

Figure 9 shows the experimental results for thermal conductivity of MWCNT/H2O-EG nanofluid samples in relation to different temperatures in a range of 20 °C-50 °C at which measurements were taken. As can be seen the thermal conductivity increases with increasing MWCNT mass fraction and temperature. The average increases were 2.25 %, 3.1 %, and 6.01% for nanofluid samples with mass concentration of 0.005 wt.%, 0.01 wt.% and 0.05 wt.% respectively. Therefore, in Fig. 8 is observed as an increment of nanofluid thermal conductivity with the increase of temperature and with the increase of the volume concentration of nanoparticles. At high temperatures, the reduction of the surface energy of the nanoparticle is favored, reducing the possibility of nanoparticle agglomeration, and causing a decrease in viscosity leading to an intensification of Brownian motion.

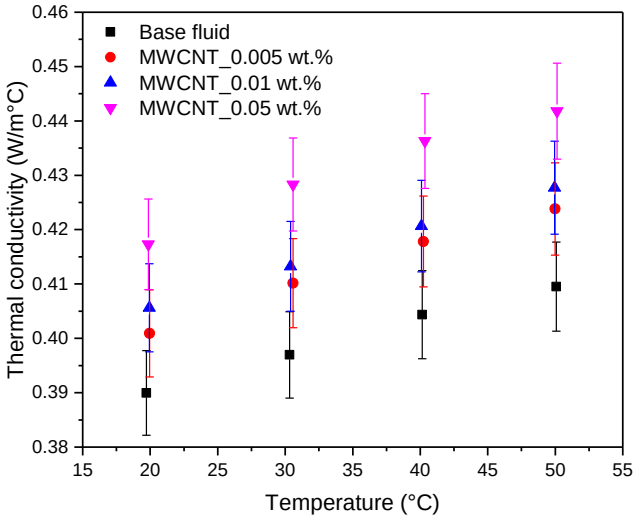

Figure 9. Thermal conductivity of MMCNT/H2O-EG nanofluid in relation to different temperatures.

Figure 10 shows a comparison of average Nusselt number of nanofluid flow in a straight pipe and a pipe with sudden geometry obtained by Montazer et al. (2020). In the straight tube the heat flux was kept constant at 10,000.00

W/m^2 and the Reynolds number varied from 500 to 10,000. For results obtained from the literature the convective heat transfer coefficient of fully developed turbulent nanofluid flowing through an abrupt enlargement with expansion ratio of 2 was evaluated at a constant heat flux of 12,128.56 W/m^2. A comparison of the results indicated an increase of almost 20 % in the Nusselt number for nanofluid with sudden geometry change. The effect of geometry is clearly seen in many studies in the literature. The results show that the Nusselt number increases with a sudden geometry change in the pipe and with the increase of Reynolds number, also the enhanced thermal conductivity and viscosity of nanofluids, as well as the random movement of nanoparticles, effect the increased enhancement of heat transfer.

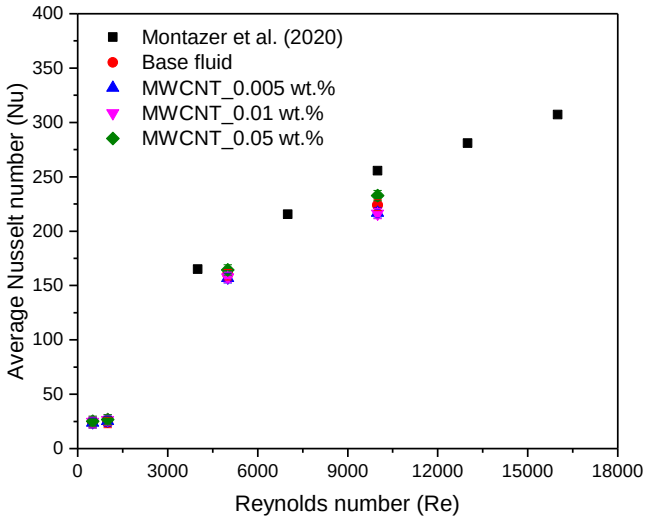

Figure 10. Comparison between average Nusselt number for MWCNT in a straight pipe and a pipe with sudden enlargement.

5. CONCLUSIONS

The results obtained of measurements for thermal conductivity of samples based on (H_2O:EG 50:50 wt.%) indicated increments above the predictions obtained by the effective means theory (EMT). Thus, the thermal conductivity of nanofluid compared to the base fluid of increased up to 9.58 %.

The viscosity of nanofluids was also another parameter experimentally determined, indicated increments slightly significative in the samples based on (H_2O:EG 50:50% wt.). At higher temperatures the increase of viscosity tends to decrease and that of thermal conductivity increases, resulting in a significant increase in thermal conductivity with a low decrease in viscosity.

Finally, the comparison between Nusselt number of nanofluid flow in a straight tube and a tube with sudden enlargement find in the literature indicate a significative increment, almost 20 % in average. Additional tests will be necessary to obtain conclusive results for heat transfer coefficient in nanofluid flow with geometry change and build a large database.

6. ACKNOWLEDGEMENTS

The authors are grateful for the financial support provided for this research by CAPES and CNPq.

7. REFERENCES

Abdulrazzaq, T., Togun, H., Goodarzi, M., Kazi, S.N., Ariffin, M.K.A., Adam, N.M., Hooman, K., 2020. “Turbulent heat transfer and nanofluid flow in an annular cylinder with sudden reduction”. *J. Therm. Anal. Calorim*. Vol. 141, pp. 373–385.

Amiri, A., Arzani, H.K., Kazi, S.N., Chew, B.T., Badarudin, A., 2016. “Backward-facing step heat transfer of the turbulent regime for functionalized graphene nanoplatelets based water-ethylene glycol nanofluids”. *Int. J. Heat Mass Transf*. Vol. 97, pp. 538–546.

Carneiro, I., Simões, S., 2020. “Effect of Morphology and Structure of MWCNTs on Metal Matrix Nanocomposites”. *Materials*, Vol. 13, No. 5557, pp. 1-16.

Dadhich, M., Prajapati, O. S., & Sharma, V., 2021. "Investigation of boiling heat transfer of titania nanofluid flowing through horizontal tube and optimization of results utilizing the desirability function approach". *Powder Technology*, Vol. 378, pp. 104 – 123.

Gómez, A.O.C., 2019. *AVALIAÇÃO EXPERIMENTAL DA TRANSFERÊNCIA DE CALOR E PERDA DE PRESSÃO DE NANOFLUIDOS EM ESCOAMENTO MONOFÁSICO EM DUTOS*. Ph.D. thesis, Universidade Federal de Uberlândia. Uberlândia, Brasil.

Hilo, A.K., Talib, A.R.A., Iborra, A.A., Sultan, M.T.H., Hamid, M.F.A., 2020. "Experimental study of nanofluids flow and heat transfer over a backward-facing step channel". *Powder Technol.* Vol. 372, pp. 497–505.

Hoffmann, A. R. K., 2014. *Análise experimental do desempenho termo-hidráulico de nanofluidos de nanotubos de carbono em escoamento monofásico*. Ph.D. thesis, Universidade Federal de Uberlândia. Uberlândia, Brasil.

Hosseinian, A., Isfahani, A. H. M., & Shirani, E., 2018. "Experimental investigation of surface vibration effects on increasing the stability and heat transfer coefficient of MWCNTs – water nanofluid in a flexible double pipe heat exchanger". *Experimental Thermal and Fluid Science*, Vol. 90, pp. 275 – 285.

Kazi, S.N., Togun, H., 2015. "Heat Transfer and Nanofluid Flow Through Different Geometries". *Heat Transf. Stud. Appl.*

Kherbeet, A.S., Mohammed, H.A., Munisamy, K.M., Saidur, R., Salman, B.H., Mahbubul, I.M., 2014. "Experimental and numerical study of nanofluid flow and heat transfer over microscale forward-facing step". *Int. Commun. Heat Mass Transf.* Vol. 57, pp. 319–329.

Kherbeet, A.S., Mohammed, H.A., Salman, B.H., Ahmed, H.E., Alawi, O.A., Rashidi, M.M., 2015. "Experimental study of nanofluid flow and heat transfer over microscale backward- and forward-facing steps". *Exp. Therm. Fluid Sci.* Vol. 65, pp. 13–21.

Kimouche, A., Mataoui, A., Oztop, H.F., Abu-Hamdeh, N., 2017. "Analysis of heat transfer of different nanofluids flow through an abrupt expansion pipe". *Appl. Therm. Eng.* Vol. 112, pp. 965–974.

Montazer, E., Shafii, M.B., Salami, E., Muhamad, M.R., Yarmand, H., Gharehkhani, S., Chowdhury, Z.Z., Kazi, S.N., Badarudin, A., 2020. "Heat transfer in turbulent nanofluids: Separation flow studies and development of novel correlations". *Adv. Powder Technol.* Vol. 31, pp. 3120–3133.

Qi, C., Ding, Z., Tu, J., Wang, Yuxing, Wang, Yinjie, 2021. "Study on backward-facing step flow and heat transfer characteristics of hybrid nanofluids". *J. Therm. Anal. Calorim.* Vol. 144, pp. 2269–2284.

Salman, S., Talib, A.R.A., Saadon, S., Sultan, M.T.H., 2020. "Hybrid nanofluid flow and heat transfer over backward and forward steps: A review". *Powder Technology*, Vol.363, pp. 448–472.

Swinehart, D.F., 1962. "The beer-lambert law". *Journal of Chemical Educationl*, Vol. 39, No. 7, pp. 333–335.

Togun, H., Kazi, S.N., Badarudin, A., 2017. "Turbulent heat transfer to separation nanofluid flow in annular concentric pipe". *Int. J. Therm. Sci.* Vol. 117, pp. 14–25.

Yang, D., Sun, B., Xu, T., Liu, B., Li, H., 2021. "Experimental and numerical study on the flow and heat transfer characteristic of nanofluid in the recirculation zone of backward-facing step microchannels". *Appl. Therm. Eng.* Vol. 199, pp. 117527.

Zhang S, Han X., 2018. "Effect of different surface modified nanoparticles on viscosity of nanofluids". *Advances in Mechanical Engineering*, Vol. 10, No 2, pp. 1-8.

8. RESPONSIBILITY NOTICE

The authors are the only responsible for the printed material included in this paper.